FUDMA Journal of Sciences (FJS)
ISSN online: 2616-1370
ISSN print: 2645 - 2944
Vol. 10 No. 24, December, 2026, pp 276 – 286
DOI: https://doi.org/10.33003/fjs-2026-1024-6545

Cross-Validated Hydro-geophysical Assessment of Basement Aquifer Characteristics, Protective Capacity and Groundwater Prospectivity across the Kabba–Aiyetoro Area, North-Central Nigeria

[*1]Momoh Jimoh Abdulsalami, [2]Joseph Omeiza Alao, [3]Fahad Abubakar, [3]Abdulmalik Onimisi Danga, [4]Muhammad Ahmad Alwali, [5]Abubakar Musa Abdullahi Fodio, [6]Michael Adewale Ibitomi and [7]Yahaya Jibrin Danjuma

[1] Department of Physics, Confluence University of Science and Technology, Osara, Kogi State, Nigeria.
[2] Department of Physics, Air Force Institute of Technology, Kaduna State, Nigeria.
[3] Department of Geosciences, Confluence University of Science and Technology, Osara, Kogi State, Nigeria.
[4] Department of Physics, Ahmadu Bello University, Zaria, Kaduna State, Nigeria.
[5] Department of Physics, University of Science and Technology, Aliero, Kebbi State, Nigeria.
[6] Department of Mineral and Petroleum Resources Engineering, Kogi State Polytechnic, Lokoja, Kogi State, Nigeria.
[7] Department of Mathematics and Statistics, Confluence University of Science and Technology, Osara, Kogi State, Nigeria.

*Corresponding authors' email: mjfati0086@gmail.com

Received: 02 Nov. 2026
Accepted: 13 Nov. 2026
Published: 16 Nov. 2026

ABSTRACT

Groundwater prospectivity in crystalline basement terrain reflects spatial variations in weathering, fracturing, aquifer geometry and overburden protection. This study integrated 20 newly acquired vertical electrical soundings (VES) extending from Kabba towards Aiyetoro, north-central Nigeria, with cross-validated spatial modelling. The 72 interpreted geoelectric layers were examined along four correlated profiles. Aquifer geometry, electrical properties and Dar Zarrouk parameters were evaluated. Hydraulic conductivity was estimated from aquifer resistivity, and transmissivity was calculated from conductivity and finite aquifer thickness. Overburden longitudinal conductance was used to classify natural protective capacity, and four normalized indicators were combined into a groundwater potential index (GPI) for 17 bounded aquifer intervals. Parameter-specific inverse distance weighting (IDW) was evaluated by leave-one-out cross-validation, with ordinary kriging comparisons for selected variables. Aquifer-top depth ranged from 1.23 to 15.38 m, bounded aquifer thickness from 0.89 to 45.20 m, and aquifer resistivity from 27.20 to 1,773.00 Ω m. Estimated transmissivity ranged from 1.18 to 245.73 m^2 day^{-1}. Protective-capacity classifications were poor at 10 stations (50%), weak at three (15%), moderate at six (30%) and good at one (5%). The GPI ranged from 0.130 to 0.750, with VES-06 (0.750), VES-14 (0.584) and VES-09 (0.574) recording the highest scores. Cross-validated normalized root-mean-square errors ranged from 20.2% to 34.7%, including 28.6% for the GPI. The assessment integrates spatially evaluated aquifer prospectivity with protective-capacity information to support groundwater investigation and source-protection planning.

Keywords: Basement aquifer, Vertical Electrical Sounding, Dar Zarrouk Parameters, Groundwater Prospectivity, Protective Capacity, Kabba–Aiyetoro

INTRODUCTION

Groundwater provides an important water supply in crystalline basement environments, where well performance can vary considerably over short distances. Groundwater storage and movement depend on the thickness and composition of weathered regolith, the extent and connectivity of basement fractures, and local geological structure. These controls produce marked spatial contrasts in aquifer productivity. Investigations in southwestern and north-central Nigeria have documented basement aquifer heterogeneity, while petrophysical studies have shown how weathering and clay content influence electrical responses (Akintorinwa et al., 2020; Akinwumiju, 2020; Mézquita González et al., 2021; Musa et al., 2023). Localized hydrogeophysical characterization is therefore central to groundwater development planning.

Vertical electrical sounding (VES) resolves layered resistivity contrasts associated with weathered and fractured basement horizons. Aquifer-top depth, thickness and resistivity describe selected groundwater-bearing intervals, while Dar Zarrouk parameters summarize the electrical response of layered materials. Studies in southwestern Nigeria have related longitudinal conductance to natural overburden protection (Akinseye et al., 2023; Tijani et al., 2021). Comparable investigations in Kogi State have combined geoelectric indices with aquifer assessment (Ameloko et al., 2022; Hudu et al., 2024). Hydraulic estimates derived from resistivity complement these indicators by supporting consistent station-level comparisons (Raji & Abdulkadir, 2022; Salih et al., 2025).

Spatial models extend discrete VES observations into mapped hydrogeophysical patterns. Groundwater prospectivity investigations have combined geophysical and geological indicators through multicriteria assessment (Ajayi et al., 2022; Kumar et al., 2022; Ogundana & Falae, 2025). The resulting maps reflect both the spatial structure of the measured properties and the interpolation settings adopted. Dabas et al. (2022) demonstrated geostatistical projection of geophysical parameters, while Ahmad et al. (2021) and Bogdan et al. (2026) compared interpolation performance

using quantitative error statistics. These studies motivate parameter-specific model selection and explicit cross-validation for spatial groundwater screening.

Investigations in north-central Nigeria provide a basis for interpreting groundwater conditions in basement terrains. Raji and Abdulkadir (2020a, 2022) evaluated groundwater-related properties of bedrock and other non-sedimentary aquifers, while their georesistivity dataset documents sounding interpretation (Raji & Abdulkadir, 2020b). Ameloko et al. (2022) assessed aquifer protection in Ajaokuta, and Musa et al. (2023) integrated geoelectrical, borehole and pumping-test information in Lokoja. Hudu et al. (2024) assessed 40 VES stations in Kabba. The present study contributes 20 independently acquired VES stations extending the investigation towards Aiyetoro and evaluates aquifer prospectivity together with protective capacity and parameter-specific spatial prediction performance.

The research addresses the integrated interpretation of aquifer geometry, electrical parameters, empirical hydraulic estimates and mapped groundwater prospectivity across the Kabba–Aiyetoro survey footprint. The relationship between aquifer prospectivity and protective overburden characteristics has practical implications for site selection and source protection (Akintorinwa et al., 2020; Opara et al., 2025). An explicitly evaluated interpolation framework further establishes the predictive performance of the derived spatial surfaces.

Accordingly, this study aims to characterize basement aquifer conditions, evaluate natural protective capacity and groundwater prospectivity, and assess the spatial prediction performance of hydrogeophysical variables across the Kabba–Aiyetoro survey area. Using 20 newly acquired vertical electrical sounding (VES) datasets, the study delineates the geoelectric architecture and lateral subsurface variations, determines aquifer geometry, electrical and Dar Zarrouk parameters, anisotropy and resistivity-derived hydraulic properties, and classifies natural aquifer protective capacity based on overburden longitudinal conductance. It further develops a composite groundwater potential index for bounded aquifer intervals, examines groundwater prospectivity alongside protective capacity, and evaluates parameter-specific spatial interpolation using inverse distance weighting, selected ordinary kriging comparisons and leave-one-out cross-validation.

MATERIALS AND METHODS

Study Area and Geological Setting

The study covers the Kabba–Aiyetoro area of Kogi State, north-central Nigeria, within a survey footprint extending approximately from 6.0448° to 6.0874°E and 7.8060° to 7.8451°N (Figure 1). The 20 newly acquired VES stations extend from Kabba towards Aiyetoro, between approximately 6.0494° and 6.0827°E and 7.8120° and 7.8406°N. The geological compilation adopts unit nomenclature from the Nigerian Geological Survey Agency (2022) Geological and Mineral Resources Map of Kogi State (1:500,000), identifying migmatite (M), gabbro and quartz gabbro including epidiorite (OGp), fine-grained flaggy quartz-biotite gneiss (Qs), and coarse-grained porphyritic biotite and biotite-hornblende granite (Su) (Figure 2). Station positions are referenced to WGS 84 (EPSG:4326), while interstation distances and interpolation use WGS 84 / UTM Zone 32N (EPSG:32632).

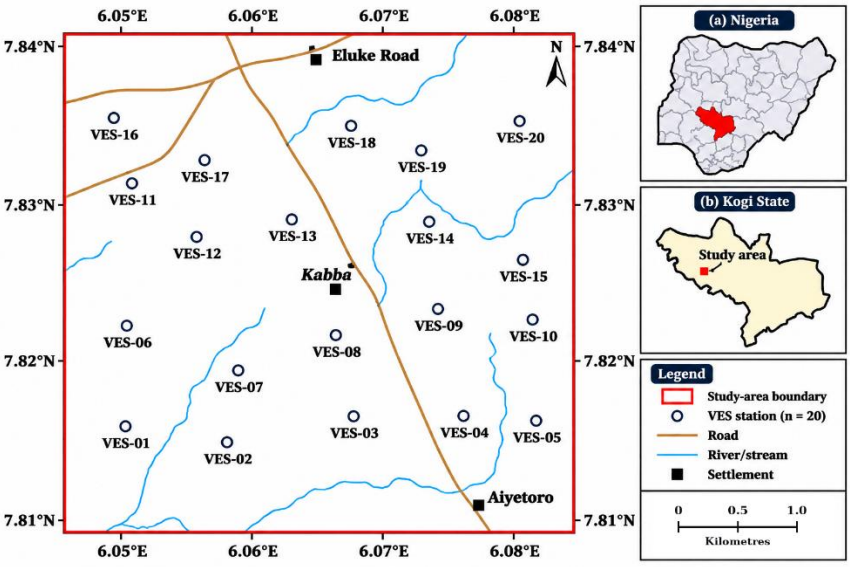


Figure 1: Location of the Kabba–Aiyetoro survey area and 20 vertical electrical sounding stations in Kogi State, Nigeria

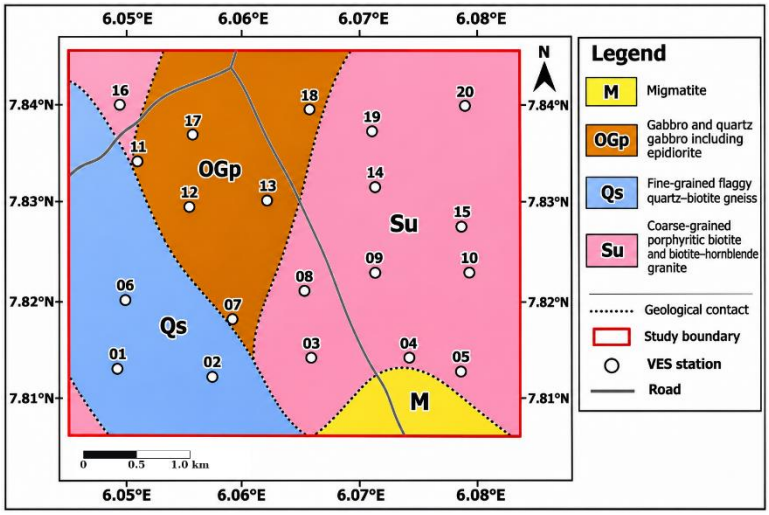


Figure 2: Geological setting and distribution of the 20 VES stations across the Kabba–Aiyetoro survey area. Geological unit nomenclature follows the Nigerian Geological Survey Agency (2022) Geological and Mineral Resources Map of Kogi State; dotted boundaries depict interpreted lithological contacts.

Research Design and Interpreted VES Dataset

A quantitative hydro-geophysical assessment was conducted using 20 newly acquired VES interpretations comprising 72 geoelectric layer records: eight three-layer and twelve four-layer models. Sounding-curve interpretation and subsequent hydro-geophysical computations were undertaken using Python scripts executed in Google Colab. The interpreted layer models contain station identifiers, WGS 84 coordinates, layer resistivities (Ω m), finite thicknesses (m), cumulative interface depths and lithological assignments. Curve types were classified from successive changes in interpreted layer resistivities and summarized in Table 1. The one-dimensional layer models provided the inputs for geoelectric profiles, Dar Zarrouk parameters, hydraulic estimates, the groundwater potential index and spatial interpolation.

Geoelectric Sections and Selection of Aquifer Intervals

Four geoelectric profiles link the five-station sequences VES-01–05 (A–A′), VES-06–10 (B–B′), VES-11–15 (C–C′) and VES-16–20 (D–D′). Projected cumulative distances locate stations along each profile, and adjoining lithological contacts were correlated from the interpreted one-dimensional models (Figure 3). Depths are expressed below local ground level. The selected groundwater-bearing layer at each station supplied the aquifer-top depth and resistivity. Seventeen stations contain finite, bounded aquifer intervals for thickness and transmissivity calculation. At VES-01, VES-03 and VES-16, the selected horizon occupies the terminal half-space; aquifer-top depth and resistivity were retained for the 20-station assessment, while thickness-dependent calculations used the 17 bounded intervals.

Dar Zarrouk Parameters and Estimated Hydraulic Properties

Total finite-layer longitudinal conductance (S_t) and transverse resistance (R) were calculated from the resistivity (ρ_i, Ω m) and thickness (h_i, m) of each finite interpreted layer above the terminal half-space. For n finite layers with summed thickness H (m), the derived longitudinal resistivity (ρL), transverse resistivity (ρT) and electrical anisotropy coefficient (λ) were computed as follows:

$$S_t = \Sigma_{i=1}^{n} (h_i / \rho_i); \quad R = \Sigma_{i=1}^{n} (h_i \rho_i) \qquad (1)$$

$$H = \Sigma_{i=1}^{n} h_i; \quad \rho L = H — S_t; \rho T = R — H;$$

$$\lambda = \sqrt{(\rho T / \rho L)} \qquad (2)$$

Hydraulic conductivity (K) was estimated from selected aquifer-layer resistivity (ρaq) using the inverse power-law expression in Equation (3). The numerical implementation follows the convention applied to north-central Nigerian basement aquifers by Raji and Abdulkadir (2022), with ρaq in Ω m and empirical K estimates reported in m day^{-1}. The expression is derived from the resistivity–conductivity relationship of Heigold et al. (1979), originally calibrated using aquifer resistivity in Ω cm and conductivity in cm s^{-1} for glacial outwash. For bounded aquifer intervals, estimated transmissivity (T, m^2 day^{-1}) was calculated from K and finite aquifer thickness b (m):

$$K = 386.4 \times \rho aq^{-0 \cdot 93283}; \quad T = Kb \qquad (3)$$

The empirical K and T estimates were derived from the interpreted geoelectric parameters using the applied resistivity convention (Heigold et al., 1979; Raji & Abdulkadir, 2022). The original and applied unit conventions are distinguished to support consistent interpretation of the resulting hydrogeophysical estimates. Station-level descriptive statistics were calculated for 20 aquifer-top depth and resistivity observations, and for the 17 finite aquifer thickness and transmissivity estimates (Table 2).

Aquifer Protective-Capacity Assessment

Natural overburden protective capacity was classified from longitudinal conductance of the layers above the selected aquifer (S_o, siemens). At each station, S_o was obtained by summing h_i/ρ_i only from the uppermost interpreted layer through the layer immediately overlying the selected aquifer top. This differs from total finite-layer conductance S_t, which includes every finite layer above the terminal half-space. The protective-capacity classes were poor ($S_o < 0.10$ S), weak ($0.10 \leq S_o < 0.20$ S), moderate ($0.20 \leq S_o < 0.70$ S) and good ($S_o \geq 0.70$ S). The station classifications are summarized in Figure 9 and Table 3, following established geoelectrical protective-capacity approaches (Akintorinwa et al., 2020; Opara et al., 2025).

Composite Groundwater Prospectivity Index

The groundwater potential index (GPI) integrates finite aquifer thickness (b), aquifer-top depth (d), resistivity-derived hydraulic conductivity (K) and overburden longitudinal conductance (S_o). It was computed for the 17 bounded aquifer intervals. For each indicator, the 2nd and 98th percentiles were calculated by linear quantile interpolation over the 17 valid station observations; the resulting scores were clipped to [0, 1]. Thickness and estimated conductivity received positive normalized scores, whereas aquifer-top depth was reverse-normalized. Positive conductance scoring integrates the natural protection of the overburden into a composite groundwater investigation priority. All four components were weighted equally (0.25 each) to provide a transparent, reproducible baseline without imposing additional expert-derived preference weights.

$$s^{+}(x) = clip\left[\frac{(x - P_2)}{(P_{98} - P_2)}, 0, 1\right]; \quad s^{-}(x) = 1 - s^{+}(x) \tag{4}$$

$$GPI = ¼\,[s^{+}(b) + s^{-}(d) + s^{+}(K) + s^{+}(S_o)] \tag{5}$$

The four normalized indicators were averaged to obtain station-level GPI scores for the 17 bounded aquifers. A sensitivity comparison was performed using an alternative three-indicator index that omitted overburden conductance and assigned equal weights to thickness, depth and estimated conductivity. Both rankings were compared with Spearman rank correlation. The four-indicator GPI was interpolated by the selected IDW model and grouped into fixed 0.20 intervals across the 0–1 scale (Figure 10). VES-01, VES-03 and VES-16 are represented separately because their selected aquifer intervals extend into terminal half-spaces.

Spatial Interpolation, Cross-Validation and Model Comparison

Spatial surfaces were estimated from the projected station coordinates on a 30 m grid within the established survey boundary. Inverse distance weighting (IDW) used an inverse-power distance function, with predicted value at location x based on the station values z_i, projected distances $d_i(x)$ and power parameter p:

$$\hat{z}(x) = [\Sigma_i\, d_i(x)^{-p}\, z_i] \,/\, [\Sigma_i\, d_i(x)^{-p}] \tag{6}$$

Candidate IDW powers p = 0.5, 1.0, 1.5, 2.0, 2.5 and 3.0 were compared by leave-one-out cross-validation (LOOCV), using all remaining stations as the prediction neighbourhood in each fold. The selected model minimized RMSE. Original-scale and applicable $\log_{10}$-transformed positive properties were evaluated with errors reported in original measurement units. For GPI, each LOOCV fold recomputed indicator percentile bounds using the 16 training stations and evaluated the held-out station with those same bounds. Overburden conductance and GPI were interpolated on the original scale using selected IDW powers of 1.5 and 2.5, respectively. Ordinary kriging with the tested linear variogram configuration was compared for longitudinal resistivity, transverse resistivity, electrical anisotropy and estimated hydraulic conductivity (Ahmad et al., 2021; Dabas et al., 2022).

Prediction errors were summarized by mean absolute error (MAE), root-mean-square error (RMSE) and range-normalized RMSE (NRMSE). The denominator for NRMSE was the observed maximum-minus-minimum range of the corresponding station parameter:

$$MAE = \left(\frac{1}{n}\right) \Sigma_i\, |z_i - \hat{z}_i|; \quad RMSE = \sqrt{[(1/n)\, \Sigma_i\, (z_i - \hat{z}_i)^2]} \tag{7}$$

$$NRMSE\ (\%) = 100 \times RMSE\ /\ (zmax - zmin) \tag{8}$$

Table 4 summarizes parameter-specific IDW cross-validation statistics. Aquifer thickness, transmissivity and the composite index use 17 bounded aquifer observations, while other properties use all 20 VES stations. The GPI validation uses fold-wise normalization with the training observations.

RESULTS AND DISCUSSION

Geoelectric Characteristics and Subsurface Architecture

The 20 VES interpretations comprise 72 layer records and six resistivity-curve types (Table 1). HA-type curves are most frequent (7 stations; 35%), followed by A and H types (4 stations each; 20% each). AA and KH each occur at two stations (10% each), while KQ occurs at one station (5%). The eight three-layer and twelve four-layer models reflect contrasting vertical resistivity sequences across the Kabba–Aiyetoro survey footprint.

Table 1: Frequency Distribution of Interpreted VES Curve Types

Curve type	Stations (n)	Percentage
A	4	20.0
AA	2	10.0
H	4	20.0
HA	7	35.0
KH	2	10.0
KQ	1	5.0

The geoelectric sections in Figure 3 identify variable topsoil and clayey cover, weathered materials, fractured basement and more resistive basement horizons. Differences in their thickness and sequence reveal pronounced lateral heterogeneity in the interpreted subsurface architecture. Correlations between adjacent VES models illustrate these changes along the four profiles.

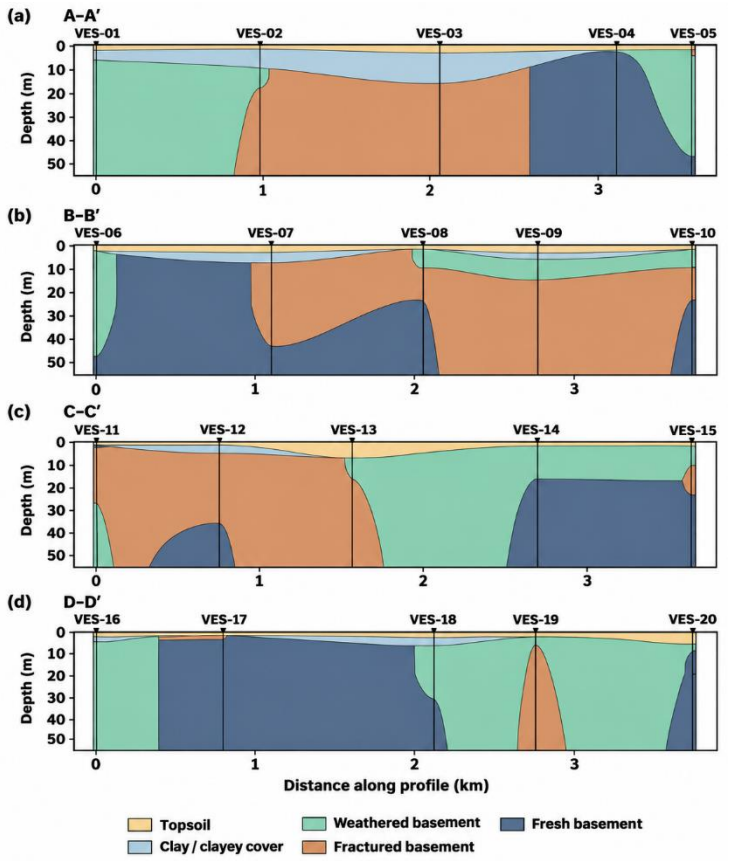


Figure 3: Interpreted two-dimensional geoelectric sections along profiles A–A′, B–B′, C–C′ and D–D′. Panels (a–d) illustrate correlated one-dimensional VES lithological interpretations. Depths are expressed below local ground level, and connections between stations are interpreted

Aquifer Geometry

Aquifer-top depth ranges from 1.23 m at VES-17 to 15.38 m at VES-03 (mean = 5.56 m; SD = 3.60 m). The interpolated surface (Figure 4) shows spatial differences in the depth of the selected groundwater-bearing horizons, reflecting variations in the near-surface geoelectric succession.

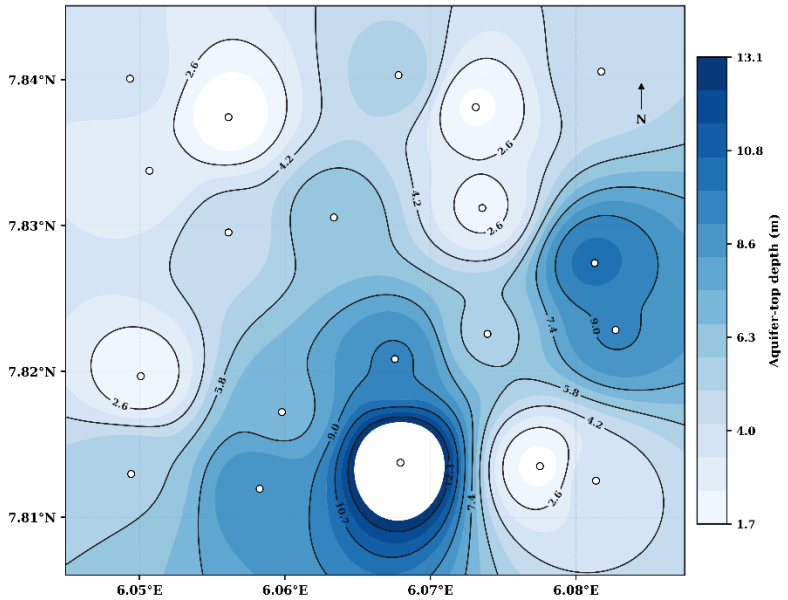


Figure 4: Spatial distribution of aquifer-top depth across the Kabba study area

Finite aquifer thickness ranges from 0.89 to 45.20 m across the 17 stations with bounded intervals (mean = 17.28 m; SD = 14.32 m). The thickest intervals are identified at VES-06 (45.20 m), VES-05 (43.40 m), VES-07 (35.30 m) and VES-12 (31.40 m). Figure 5 presents the interpolated thickness pattern, and Table 2 summarizes the station-level values.

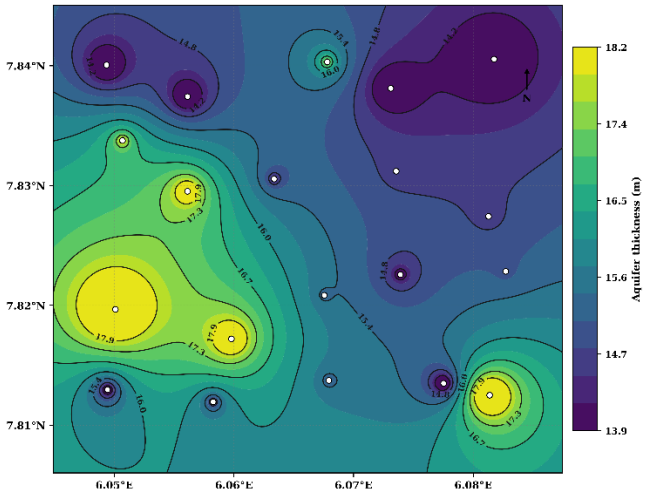


Figure 5: Spatial distribution of interpreted aquifer thickness across the Kabba study area

Table 2: Descriptive Statistics of Selected Geoelectric and Inferred Hydraulic Parameters

Parameter	Unit	n	M	SD	Range
Aquifer-top depth	m	20	5.56	3.60	1.23–15.38
Finite aquifer thickness	m	17	17.28	14.32	0.89–45.20
Aquifer resistivity	Ω m	20	467.51	496.50	27.20–1,773.00
Overburden longitudinal conductance	S	20	0.194	0.264	0.005–1.178
Transverse resistance	Ω m²	20	9,465.53	15,125.98	120.33–56,618.82
Longitudinal resistivity	Ω m	20	177.30	311.39	13.06–1,432.91
Transverse resistivity	Ω m	20	350.77	501.81	29.33–2,091.57
Anisotropy coefficient	—	20	1.40	0.35	1.01–2.39
Estimated hydraulic conductivity	m day⁻¹	20	4.82	5.45	0.36–17.73
Estimated transmissivity	m² day⁻¹	17	67.36	80.88	1.18–245.73
Composite groundwater score	—	17	0.383	0.178	0.130–0.750

Electrical Properties and Inferred Hydraulic Characteristics

Aquifer resistivity ranges from 27.20 to 1,773.00 Ω m (mean = 467.51 Ω m; SD = 496.50 Ω m). The spatial distribution in Figure 6 illustrates pronounced electrical contrasts among the interpreted target intervals, consistent with differences in weathering, fracturing, clay content and pore-water conductivity.

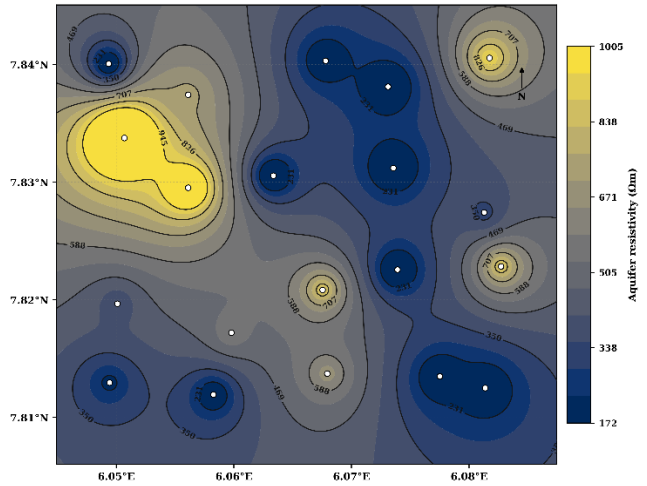


Figure 6: Spatial distribution of interpreted aquifer resistivity across the Kabba study area
Note: Aquifer resistivity is expressed in ohm-metres (Ω m). Open circles denote VES locations.

Longitudinal resistivity ranges from 13.06 to 1,432.91 Ω m, transverse resistivity from 29.33 to 2,091.57 Ω m and electrical anisotropy from 1.01 to 2.39 (mean = 1.40). Transverse resistance ranges from 120.33 to 56,618.82 Ω m². These parameters characterize contrasts within the layered geoelectric models (Figure 7). Estimated hydraulic conductivity ranges from 0.36 to 17.73 m day⁻¹ (mean = 4.82 m day⁻¹).

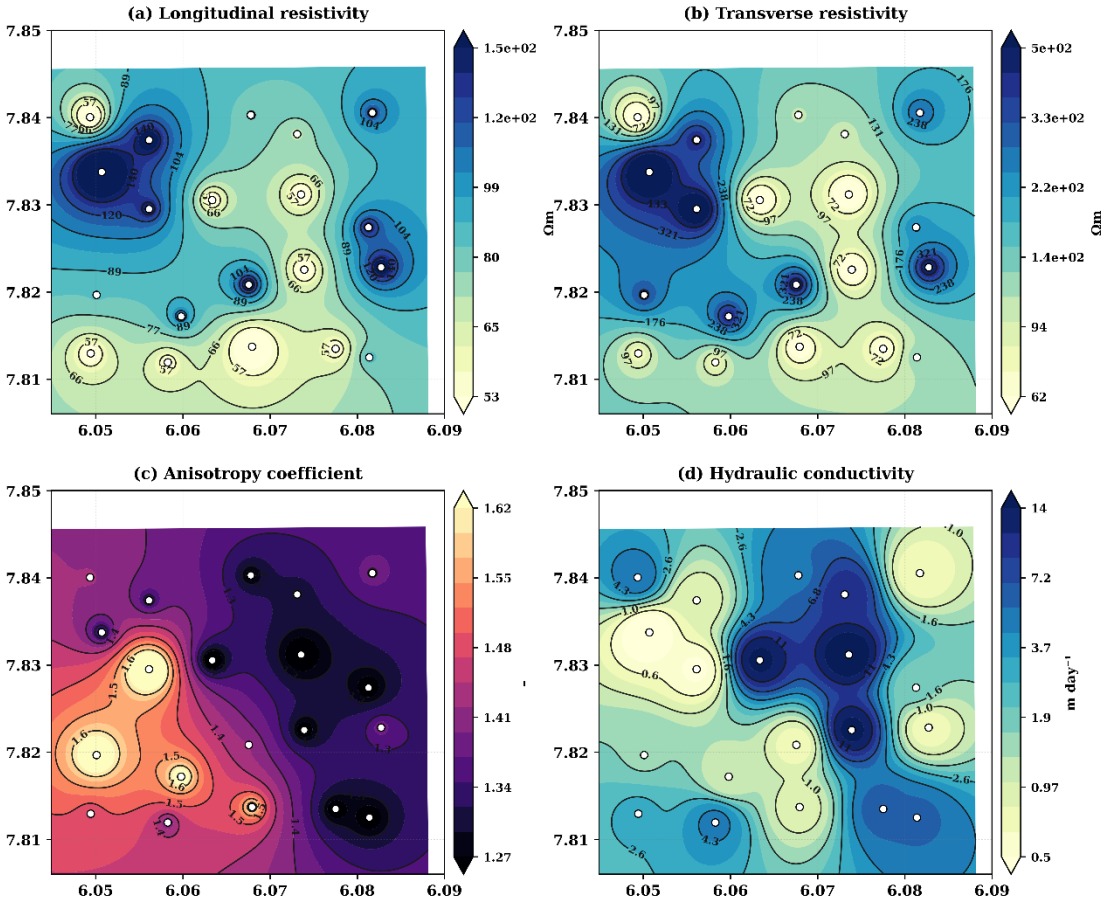


Figure 7: Spatial variation in longitudinal resistivity, transverse resistivity, electrical anisotropy and estimated hydraulic conductivity

Note: Panels (a–d) show longitudinal resistivity (Ω m), transverse resistivity (Ω m), coefficient of anisotropy (dimensionless) and estimated hydraulic conductivity (m day⁻¹), respectively.

Estimated transmissivity across the 17 bounded aquifer intervals ranges from 1.18 to 245.73 m² day⁻¹ (mean = 67.36 m² day⁻¹; SD = 80.88 m² day⁻¹). The highest station estimates occur at VES-05 (245.73 m² day⁻¹), VES-14 (235.87 m² day⁻¹), VES-13 (147.79 m² day⁻¹), VES-18 (131.09 m² day⁻¹) and VES-09 (128.36 m² day⁻¹). The interpolated pattern is presented in Figure 8. Differences in estimated conductivity and interpreted thickness jointly account for the variation in computed transmissivity.

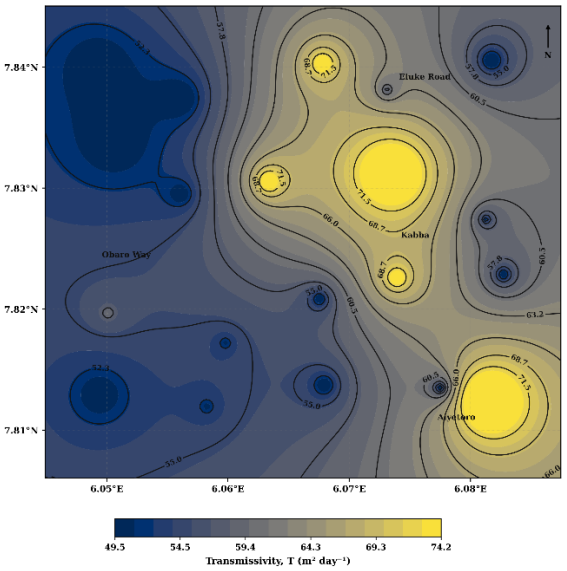


Figure 8: Spatial distribution of estimated aquifer transmissivity across the Kabba study area
Note: Transmissivity is expressed in m^2 day^{-1} and calculated from resistivity-derived hydraulic conductivity and interpreted aquifer thickness.

Natural Aquifer Protective Capacity

Overburden longitudinal conductance ranges from 0.005 to 1.178 S (mean = 0.194 S; SD = 0.264 S). The corresponding natural protective-capacity assessment identifies 10 poor stations (50%), three weak stations (15%), six moderate stations (30%) and one good station (5%). Figure 9 presents the threshold-classified interpolated conductance together with station classifications; Table 3 summarizes the station-based distribution. VES-03 records the highest overburden conductance (1.178 S), while VES-11 records the lowest (0.005 S).

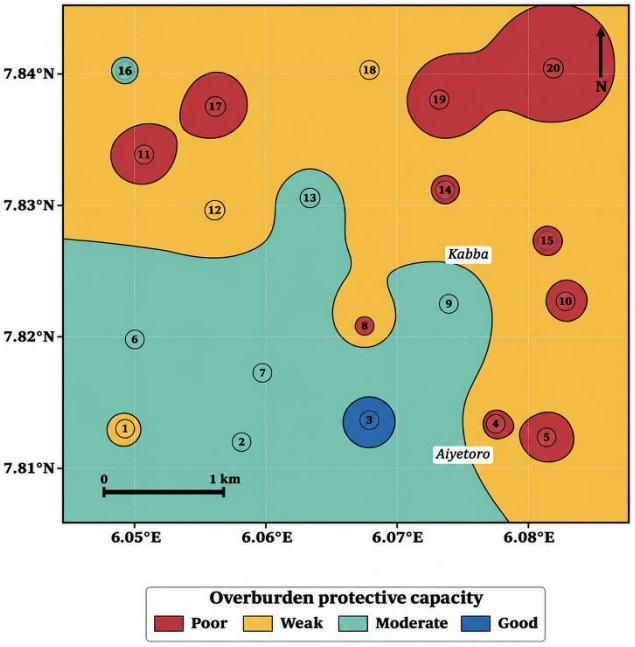


Figure 9: Spatial distribution of aquifer protective-capacity classes in the Kabba study area
Note: Protective-capacity classes are derived from interpreted longitudinal conductance and shown as poor, weak, moderate and good.

Table 3: Station-Based Aquifer Protective-Capacity Classes

Class	n	Percentage	Conductance range (S)
Poor	10	50.0	0.005–0.081
Weak	3	15.0	0.155–0.169
Moderate	6	30.0	0.219–0.432
Good	1	5.0	1.178

Note: S denotes longitudinal conductance in siemens. Percentages are based on 20 VES stations.

Composite Groundwater Prospectivity

The recalculated GPI spans 0.130–0.750 across the 17 bounded aquifer intervals (mean = 0.383; SD = 0.178). VES-06 (0.750), VES-14 (0.584), VES-09 (0.574), VES-13 (0.521) and VES-05 (0.517) record the five highest composite scores. Figure 10 presents the interpolated GPI and the station-level scores within fixed index classes. The separate representation of the three terminal aquifer intervals maintains consistency between the thickness-dependent index and the interpreted layer geometry.

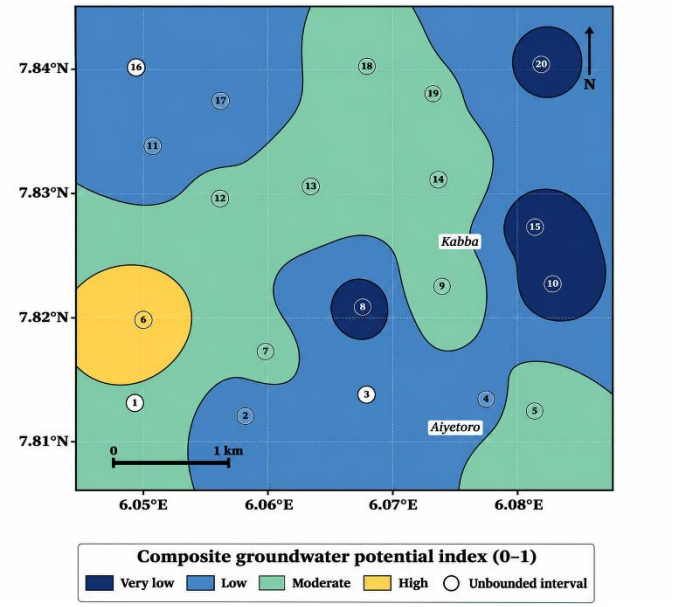


Figure 10: Groundwater prospectivity map of the Kabba study area based on the composite groundwater potential index
Note: The map presents relative groundwater potential classes derived from the integrated VES-based index.

Spatial Interpolation and Validation

Selected IDW powers range from 0.5 to 3.0 across the ten assessed parameters (Table 4). Leave-one-out normalized root-mean-square errors (NRMSE) range from 20.2% for aquifer-top depth to 34.7% for estimated transmissivity. Overburden conductance yields RMSE = 0.262 S (NRMSE = 22.3%) at p = 1.5, matching Table 4. For the 17-station GPI, fold-wise normalization gives RMSE = 0.177 (NRMSE = 28.6%) at p = 2.5. In the four selected comparisons, IDW produces slightly lower RMSE than the tested linear-variogram ordinary kriging configurations.

Table 4: IDW Leave-One-Out Cross-Validation of Selected Ves-Derived Parameters

Parameter	n	Power	MAE	RMSE	NRMSE (%)
Aquifer-top depth	20	3	2.198	2.862	20.2
Finite aquifer thickness	17	0.5	12.534	14.863	33.5
Aquifer resistivity	20	1.5	422.351	501.225	28.7
Overburden longitudinal conductance	20	1.5	0.165	0.262	22.3
Estimated transmissivity	17	0.5	71.290	84.746	34.7
Longitudinal resistivity	20	1	148.031	321.323	22.6
Transverse resistivity	20	1.5	312.870	529.915	25.7
Electrical anisotropy	20	1	0.261	0.348	25.2
Estimated hydraulic conductivity	20	3	3.685	5.638	32.4
Composite groundwater score	17	2.5	0.144	0.177	28.6

Interpretation of the Findings

Basement Aquifer Architecture and Electrical Heterogeneity

The seven HA-type curves and variations across the four geoelectric profiles illustrate the heterogeneous weathering and fracture characteristics of the Kabba–Aiyetoro basement. Similar vertical and lateral variability has been described by Akinwumiju (2020) and Akintorinwa et al. (2020) in southwestern Nigerian crystalline terrain. Hudu et al. (2024) examined 40 VES stations in Kabba, whereas the present 20-station independent survey extends geographical coverage towards Aiyetoro and adds parameter-specific cross-

validation to the joint interpretation of prospectivity and overburden protection.

Implications of Aquifer Geometry and Inferred Hydraulic Parameters

Estimated transmissivity reflects the combined contribution of interpreted aquifer thickness and resistivity-derived conductivity. VES-06 has the thickest bounded interval (45.20 m), while VES-14 combines a 13.30 m interval with the highest calculated conductivity (17.73 m day^{-1}). Their estimated hydraulic characteristics support comparisons among the surveyed locations. The inverse resistivity–conductivity form originates from Heigold et al. (1979), while Raji and Abdulkadir (2022) demonstrate its applied use in north-central Nigerian basement aquifers; related regional investigations likewise integrate geoelectric parameters for aquifer characterization (Tijani et al., 2021; Salih et al., 2025).

Groundwater Prospectivity in Relation to Natural Protective Capacity

Groundwater prospectivity and overburden protective capacity contribute complementary information to groundwater planning. The 17-station GPI combines interpreted aquifer geometry, empirical hydraulic estimates and overburden conductance; the 20-station protective-capacity classification identifies 13 stations (65%) within the poor and weak categories. VES-06 ranks first in GPI and has moderate overburden protection; VES-14 ranks second with poor protection; VES-09 ranks third with moderate protection. In the sensitivity assessment, the four-indicator ranking and the alternative three-indicator ranking show a Spearman correlation of 0.870 (n = 17). This indicates substantial agreement in overall station order while highlighting how the protection indicator influences individual priorities. The combined interpretation supports targeted aquifer investigation and source-protection planning (Akintorinwa et al., 2020; Hudu et al., 2024; Opara et al., 2025).

Interpretation of Spatial Model Performance

LOOCV provides parameter-specific evidence of map prediction performance: NRMSE ranges from 20.2% to 34.7%, corresponding to larger errors for transmissivity than for aquifer-top depth. The 17-station GPI attains 28.6% NRMSE with fold-wise normalization, while overburden conductance attains 22.3%. These results provide an explicit basis for comparing candidate interpolation settings for each hydrogeophysical property. IDW gives marginally lower RMSE than the four tested ordinary kriging configurations, a comparison consistent with parameter-dependent performance reported in spatial interpolation studies (Ahmad et al., 2021; Bogdan et al., 2026; Dabas et al., 2022).

Scientific Contribution and Groundwater Management Relevance

This investigation extends the hydrogeophysical evidence from Kabba towards Aiyetoro through 20 newly acquired VES interpretations and integrates geoelectric architecture, Dar Zarrouk parameters, estimated hydraulic properties, protective overburden characteristics and prospectivity assessment. Its contribution is strengthened by parameter-specific spatial interpolation and quantitative cross-validation. The combined station-level assessment identifies groundwater investigation priorities and areas requiring attention to natural source protection.

Conclusion

This study integrated 20 newly acquired vertical electrical soundings, geoelectric sections, Dar Zarrouk parameters and cross-validated spatial modelling to characterize basement aquifer conditions across Kabba towards Aiyetoro in north-central Nigeria. The interpreted profiles demonstrate variations in the geometry and electrical properties of groundwater-bearing horizons. Aquifer-top depth ranges from 1.23 to 15.38 m, while finite aquifer thickness varies from 0.89 to 45.20 m across 17 bounded intervals. Aquifer resistivity ranges from 27.20 to 1,773.00 Ω m, and resistivity-derived transmissivity ranges from 1.18 to 245.73 m² day^{-1}.

Overburden protective capacity is classified as poor at 10 stations (50%), weak at three (15%), moderate at six (30%) and good at one (5%). The groundwater potential index ranges from 0.130 to 0.750 across the 17 bounded aquifer intervals. VES-06, VES-14 and VES-09 record the highest index scores and exhibit different protective-capacity characteristics that inform integrated groundwater investigation and source-protection priorities.

Parameter-specific inverse distance weighting and leave-one-out cross-validation produce normalized root-mean-square errors of 20.2–34.7% across the analysed variables. The study provides a quantitatively evaluated groundwater assessment framework connecting geoelectric architecture, empirical hydraulic estimates, protective capacity and groundwater prospectivity. Future research should prioritize borehole investigations, pumping tests and groundwater-quality assessment around VES-06, VES-14 and VES-09 to refine site-scale hydraulic characterization and support groundwater source-protection planning.

REFERENCES

Ahmad, A. Y., Saleh, I. A., Balakrishnan, P., & Al-Ghouti, M. A. (2021). Comparison of GIS-based interpolation methods for mapping groundwater quality in the state of Qatar. Groundwater for Sustainable Development, 13, 100573. https://doi.org/10.1016/j.gsd.2021.100573

Ajayi, O. G., Nwadialor, I. J., Odumosu, J. O., Adetunji, O. O., & Abdulwasiu, I. O. (2022). Assessment and delineation of groundwater potential zones using integrated geospatial techniques and analytic hierarchy process. *Applied Water Science, 12*, Article 276. https://doi.org/10.1007/s13201-022-01802-4

Akinseye, V. O., Osisanya, W. O., Eyankware, M. O., Korode, I. A., & Ibitoye, A. T. (2023). Application of second-order geoelectric indices in determination of groundwater vulnerability in hard rock terrain in SW. Nigeria. *Sustainable Water Resources Management, 9*, Article 169. https://doi.org/10.1007/s40899-023-00936-w

Akintorinwa, O. J., Atitebi, M. O., & Akinlalu, A. A. (2020). Hydrogeophysical and aquifer vulnerability zonation of a typical basement complex terrain: A case study of Ododе Idanre southwestern Nigeria. *Heliyon, 6(8)*, e04549. https://doi.org/10.1016/j.heliyon.2020.e04549

Akinwumiju, A. S. (2020). Hydrogeological characteristics of crystalline rock aquifers: Implication on sustainable water supply in the basement complex terrain of southwestern Nigeria. *Sustainable Water Resources Management, 6*, 26. https://doi.org/10.1007/s40899-020-00381-z

Ameloko, A. A., Obihan, I., Onugba, A., Ajayi, G., Rotimi, O. J., & Okezie, U. (2022). Geophysical investigation of

aquifer vulnerability and protective capacity of overburden rocks in part of Ajaokuta, Kogi State, North Central, Nigeria. *Sustainable Water Resources Management, 8*, Article 102. https://doi.org/10.1007/s40899-022-00681-6

Bogdan, P.-L., Nedeff, V., Panainte-Lehadus, M., Chițimuș, A.-D., Barsan, N., Nedeff, F. M., & López-Ramírez, J. A. (2026). Evaluation of selected geostatistical methods for interpolating hydraulic conductivity in shallow alluvial aquifers using cross-validation statistics. *Water, 18(15)*, 1876. https://doi.org/10.3390/w18151876

Dabas, J., Sarah, S., Mondal, N. C., & Ahmed, S. (2022). Geostatistical spatial projection of geophysical parameters for practical aquifer mapping. *Scientific Reports, 12*, 4641. https://doi.org/10.1038/s41598-022-08494-5

Heigold, P. C., Gilkeson, R. H., Cartwright, K., & Reed, P. C. (1979). Aquifer transmissivity from surficial electrical methods. Ground Water, 17(4), 338–345. https://doi.org/10.1111/j.1745-6584.1979.tb03326.x

Hudu, A. S., Fabian, A. A., Kizito, O. M., & Jacob, B. J. (2024). Application of primary and secondary resistivity parameters in evaluating aquifer potential and vulnerability within Kabba, North Central Nigeria. *FUDMA Journal of Sciences, 8(4)*, 221–234. https://doi.org/10.33003/fjs-2024-0804-2581

Kumar, G., Kumar, D., & Warwade, P. (2022). GIS and geophysics: An integrative and inter-evaluating approach towards groundwater assessment. *Geocarto International, 37(27)*, 15656–15682. https://doi.org/10.1080/10106049.2022.2102220

Mézquita González, J. A., Comte, J.-C., Legchenko, A., Ofterdinger, U., & Healy, D. (2021). Quantification of groundwater storage heterogeneity in weathered/fractured basement rock aquifers using electrical resistivity tomography: Sensitivity and uncertainty associated with petrophysical modelling. *Journal of Hydrology, 593*, Article 125637. https://doi.org/10.1016/j.jhydrol.2020.125637

Musa, K. O., Obasi, I. A., Auduson, A. E., Jatto, S. S., Akudo, E. O., Akpah, F., & Jimoh, J. B. (2023). Integrating geoelectrical and borehole data in the characterization of basement-rock aquifers in the Lokoja area, northcentral Nigeria. *Geosystems and Geoenvironment, 2(4)*, 100217. https://doi.org/10.1016/j.geogeo.2023.100217

Nigerian Geological Survey Agency. (2022). Geological and mineral resources map of Kogi State, Nigeria [Map, scale 1:500,000]. https://ngsa.gov.ng/wp-content/uploads/2024/08/Kogi-State-Mineral-Resources-Map-2022.pdf

Ogundana, A. K., & Falae, P. O. (2025). Groundwater potential modelling and aquifer zonation of a typical basement complex terrain: A case study. *Environment, Development and Sustainability, 27(12)*, 31081–31103. https://doi.org/10.1007/s10668-024-04940-8

Opara, A. I., Ireaja, A. N., Eyankware, M. O., Urom, O. O., Ikoro, D. O., Akakuru, O. C., Dioha, E., & Omoko, N. E. (2025). A critical analysis of the comparative techniques of aquifer protective capacity studies in part of Southeastern Nigeria. *International Journal of Energy and Water Resources, 9(2)*, 653–685. https://doi.org/10.1007/s42108-023-00251-2

Raji, W. O., & Abdulkadir, K. A. (2020a). Evaluation of groundwater potential of bedrock aquifers in Geological Sheet 223 Ilorin, Nigeria, using geo-electric sounding. *Applied Water Science, 10*, Article 220. https://doi.org/10.1007/s13201-020-01303-2

Raji, W. O., & Abdulkadir, K. A. (2020b). Geo-resistivity data set for groundwater aquifer exploration in the basement complex terrain of Nigeria, West Africa. *Data in Brief, 31*, Article 105975. https://doi.org/10.1016/j.dib.2020.105975

Raji, W. O., & Abdulkadir, K. A. (2022). Quantitative estimates of groundwater resource parameters in non-sedimentary aquifers of Northcentral Nigeria. *Journal of African Earth Sciences, 196*, 104695. https://doi.org/10.1016/j.jafrearsci.2022.104695

Salih, S., Azagegen, T., Haile, T., & Fentaw, B. (2025). Determination of hydraulic properties from geoelectrical parameters in Raya Valley aquifer, Northern Ethiopia. *Journal of Hydrology: Regional Studies, 62*, 103002. https://doi.org/10.1016/j.ejrh.2025.103002

Tijani, M. N., Obini, N., & Inim, I. J. (2021). Estimation of aquifer hydraulic parameters and protective capacity in basement aquifer of south-western Nigeria using geophysical techniques. *Environmental Earth Sciences, 80*, 466. https://doi.org/10.1007/s12665-021-09759-4

©2026 This is an Open Access article distributed under the terms of the Creative Commons Attribution 4.0 International license viewed via https://creativecommons.org/licenses/by/4.0/ which permits unrestricted use, distribution, and reproduction in any medium, provided the original work is cited appropriately.